In Vivo Confocal Microscopy Morphometric Analysis of Meibomian Glands in Patients With Graves Ophthalmopathy

Aldo Vagge, MD, PhD, Federico Bernabei, MD,† Chiara Del Noce, MD,* Marco Pellegrini, MD,† Giuseppe Giannaccare, MD, PhD,‡ Carlotta Senni, MD,† Riccardo Scotto, PhD,* and Carlo E. Traverso, MD**

Purpose: To characterize meibomian glands (MGs) features in patients with Graves ophthalmopathy (GO) by in vivo confocal microscopy (IVCM) and to further investigate possible correlations with ocular surface characteristics.

Methods: Consecutive patients with GO and controls were enrolled. The following ocular surface parameters were measured: tear break-up time, Schirmer test, and corneal fluorescein staining (Oxford score) were performed on each subject. IVCM of MGs was performed, and the scans were analyzed with ImageJ software for the calculation of the following: acinar unit density, total gland area, total lumen area (TLA), acinar longest diameter, and acinar shortest diameter. A nonparametric Mann–Whitney *U* test was used to compare variables between patients with GO and controls. The Spearman correlation analysis was used to evaluate the correlations between ocular surface and IVCM parameters.

Results: Twenty-one patients with GO and 24 sex- and age-matched healthy controls were included. Acinar unit density was significantly lower in patients with GO compared with controls (24.5 ± 8.1 vs. 34.2 ± 7.5 U/mm^2; $P < 0.001$). In addition, patients with GO showed significantly higher values of TLA, acinar longest diameter, and acinar shortest diameter compared with controls (respectively, 3104.7 ± 1713.3 vs. 1393.8 ± 448.0 μm^2, 94.4 ± 21.2 vs. 64.3 ± 10.1 μm and 56.6 ± 15.3 vs. 42.2 ± 12.3 μm; always $P < 0.05$). In patients with GO, TLA showed a significant inverse correlation with Schirmer test (Rs = −0.467; $P = 0.038$).

Conclusions: IVCM allowed to detect distinctive features of MGs in patients with GO and could represent a surrogate tool for the assessment of MG status in these patients.

From the *Department of Neuroscience, Rehabilitation, Ophthalmology, Genetics, Maternal and Child Health (DiNOGMI), Eye Clinic of Genoa, Policlinico San Martino, University of Genova, Genova, Italy; †Ophthalmology Unit, S. Orsola-Malpighi Hospital, Bologna, Italy; and ‡Department of Ophthalmology, University Magna Græcia of Catanzaro, Catanzaro, Italy.

The authors have no funding or conflicts of interest to disclose.

A. Vagge and F. Bernabei Shared co-first authorship.

Correspondence: Aldo Vagge, MD, PhD, University Eye Clinic of Genoa DiNOGMI, University of Genoa, IRCCS Ospedale Policlinico San Martino Viale Benedetto XV, 5 16132 Genova (GE), Italy (e-mail: aldo.vagge@unige.it).

Key Words: meibomian glands, in vivo confocal microscopy, Graves ophthalmopathy, meibomian gland dysfunction, ocular surface

Graves–Basedow disease is an autoimmune thyroid disorder in which activating thyrotropin–receptor antibodies induce thyroid hormone overproduction, resulting in hyperthyroidism and goiter.[1] Graves ophthalmopathy (GO) is the most frequent extrathyroidal expression, affecting about half of overall patients.[2] GO consists of an immune-mediated inflammation, affecting orbital adipose, connective tissues, extraocular muscles, and lacrimal gland. The most common clinical features include upper eyelid retraction, periorbital edema, conjunctival chemosis, proptosis, lagophthalmos, restrictive myopathy, compressive optic neuropathy, and dry eye disease (DED).[3] The origin of DED in patients with GO is multifactorial, and different factors among T-cell–mediated inflammation of the lacrimal gland, proptosis, and lid fissure widening may contribute, to various extents, to its onset and progression.[4–7] Previous studies characterized ocular surface parameters in patients with GO, reporting the alterations of Schirmer test, corneal staining, corneal sensitivity, and goblet cell density.[4–7] Furthermore, Kocabeyoglu et al[8] showed the presence of inflammatory signs at the ocular surface even in newly diagnosed Graves patients without any evidence of active GO.

Meibomian gland dysfunction (MGD) has been proposed as an additional causing factor of DED in patients with GO.[4,9–12] Therefore, a comprehensive assessment of morphology and function of meibomian glands (MGs) based on slit-lamp examination of lid margin, evaluation of meibum quality and expressibility, tear break-up time (TBUT), lipid layer thickness (LLT), and noncontact meibography has been included in the diagnostic workup of patients with GO.[4,10–12] In vivo confocal microscopy (IVCM) represents a further tool for the high-resolution assessment at a cellular level of various ocular surface structures, including MGs.[13,14] To date, IVCM has been mainly used in patients with GO to evaluate the features of corneal and conjunctival epithelia and corneal subbasal nerve plexus.[15,16] The aim of the present study was to investigate MGs features in patients with GO by means of IVCM and to further correlate IVCM findings with ocular surface parameters.

PATIENT METHODS

Study Design and Participants

This cross-sectional observational study was conducted between January and September 2018 at the University Eye Clinic of Genoa, Policlinico San Martino, Department of Neuroscience, Rehabilitation, Ophthalmology, Genetics, Maternal and Child Health (DiNOGMI), Genoa, Italy. The study was performed in accordance with the principles of the tenets of the Declaration of Helsinki and received approval from the institutional review board. Consecutive patients with GO who presented at the ocular surface office for routine evaluation were included. Healthy sex- and age-matched subjects undergoing routine eye examination acted as controls. The exclusion criteria for both groups included previous ocular surgery, glaucoma, ocular surface disease other than GO, and any usage of eye drops within 1 month before the study initiation.

Ophthalmological Examination

Slit-lamp examination with ocular surface staining was performed after the administration of 2 μL of 2% fluorescein dye using the blue cobalt filter and a 7503 Boston yellow filter kit to enhance staining details. Corneal staining was graded according to the Oxford scale: from 0 = none to 5 = extended areas of confluent stain.[17] Schirmer test type I and TBUT measurements were performed according to the Dry Eye Workshop II guidelines.[18] The activity of GO was assessed by using the Clinical Activity Score (CAS) that is based on typical signs and symptoms of inflammation as follows: spontaneous pain, pain when moving the eye, swelling of eyelids, redness of eyelids, conjunctival injection, chemosis, swelling of plica/caruncle, increase in proptosis, and decrease in eye movement or in visual acuity. For each item, 1 point is given, for a maximum score of 10.[19]

In Vivo Confocal Microscopy

All participants underwent laser IVCM using a Heidelberg Retina Tomograph 3 with the Rostock Cornea Module (Heidelberg Engineering, Heidelberg, Germany). An experienced operator (A.V.) masked to the patients' characteristics performed all the IVCM examinations. Two-dimensional images, covering a 400 × 400 μm area, were obtained. When the first superficial conjunctival cells were visualized, the pachymetry was set at zero and the focal plane was moved to reach the subconjunctival tissue where the MGs acini could be visualized, usually at a depth of 20 to 70 μm below the epithelial surface. MGs were scanned moving horizontally from the nasal to temporal eyelid section. Digital images were recorded with the sequence mode at a rate of 3 frames per second, including 100 images per sequence. A total of 6 to 8 sequence scans of nonoverlapping areas were recorded focusing on MGs. Three nonoverlapping, high-quality digital images of the nasal, middle, and temporal lower eyelid (total of 9 images per eyelid) were selected by 2 masked examiners (C.D.N., R.S.) and used for the analysis.

Digital Image Analysis

The images were analyzed using the public domain software ImageJ 1.51 s (National Institutes of Health, Bethesda, MD, available: http://rsb.info.nih.gov/ij/) using a modified technique that was previously described.[20] Briefly, each 400 × 400-μm frame was opened in ImageJ, and the multipoint tool was used to evaluate the number of clearly visible acinar unit per image, then the acinar unit density (AUD) per mm^2 was calculated. Subsequently, the polygon tool was used to trace and measure MGs acinar unit area and lumen area, then the total gland area and the total lumen area (TLA) per mm^2 were calculated. Finally, the straight-line selection tool was used to trace and measure the acinar longest diameter (ALD) and the acinar shortest diameter (ASD). The mean value of each parameter was used for the analysis. Representative IVCM images of a healthy subject analyzed with ImageJ software is shown in Figures 1A, B.

Statistical Analysis

Statistical analysis was conducted with SPSS statistical software (SPSS Inc, Chicago, IL). Values are expressed as mean ± SD. The nonparametric Mann–Whitney *U* test was used to compare variables between the GO group and the control group. The Spearman correlation analysis was used to evaluate the correlations between ocular surface and IVCM parameters. *P* value <0.05 was considered statistically significant.

RESULTS

A total of 21 patients with GO (mean CAS 3.1 ± 2.1) and 24 healthy controls were enrolled. The demographic and

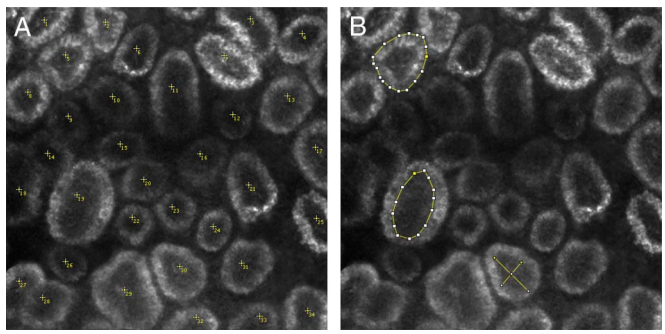

FIGURE 1. Representative in vivo confocal microscopy (IVCM) image of meibomian glands (MGs) in a healthy subject analyzed with different ImageJ tools. Mean acinar unit densities, areas, and diameters were calculated from a total of 9 IVCM images obtained from the lower lid of the subject. A, The multipoint tool was used to evaluate the number of clearly visible acinar unit. The mean AUD was 83.4 ± 8.3 U/mm^2. B, The polygon tool was used to trace and measure MGs acinar unit area (top left) and lumen area (bottom left). The total gland area and the TLA were 4325.2 ± 2942.2 μm^2 and 1452.2 ± 672.3 μm^2, respectively. The straight-line selection tool was used to trace and measure the acinar longest and shortest diameters (bottom center). The mean longest and shortest acinar unit diameters were 42.5 ± 12.3 μm and 22.4 ± 6.2 μm, respectively.

clinical characteristics of subjects included in the study are reported in Table 1. No significant differences in age and sex distribution between patients with GO and control subjects were observed (always $P > 0.05$). Patients with GO showed significantly lower values of Schirmer test, TBUT, and higher value of Oxford score compared with control subjects (always $P < 0.05$).

Table 2 shows MGs parameters calculated with IVCM in patients with GO and control subjects. The AUD was significantly lower in patients with GO compared with controls ($P < 0.001$). Patients with GO showed a significantly higher values of TLA, ALD, and ASD compared with controls (always $P < 0.05$). Representative IVCM images collected from a healthy subject and a GO patient are shown in Figures 2A, B.

In patients with GO, TLA showed a significant correlation with Schirmer test (Rs = −0.467; $P = 0.038$), whereas ASD showed a significant correlation with TBUT (Rs = 0.600; $P = 0.005$). No significant correlations between CAS score and IVCM parameters were found (always $P > 0.05$).

DISCUSSION

In the present study, we evaluated MGs microstructure in patients with GO using IVCM. Interestingly, patients with GO showed a significant lower AUD compared with control subjects. In addition, patients with GO exhibited bigger MGs, as demonstrated by the higher values of TLA, ALD, and ASD.

The presence of bigger and enlarged glands may be explained, as suggested by the International Workshop on MGD, by the high prevalence of obstructed MGs.[21]

In patients with GO, the incomplete blinking secondary to lid fissure widening and proptosis might decrease the excretion rate of the meibum. A previous report showed that patients with lagophthalmos and lid retraction secondary to facial peripheral nerve palsy present a decreased excretion of the MGs with a worsening of MGD.[22] It can be assumed that the same pathogenetic mechanism may also occur in patients with GO. The stasis of meibum inside the gland results in a cascade of events such as obstruction, increased pressure, dilation, and acinar atrophy, which in turn causes low meibum secretion. This phenomenon may explain also the higher MGs loss affecting the upper eyelids that are more likely affected by blinking compared with the lower ones as demonstrated by Park and Baek[4] using meibography examination. In fact, the upper eyelids are characterized by a larger area with a higher exposure to the inflammatory mediators present on the ocular surface. In addition, because the upper eyelids perform wider movements, particularly in patients with GO with lid fissure widening and proptosis, they are exposed to a greater mechanical stress during the blinking cycle.[4]

In addition to obstruction, inflammation process itself can directly affect MGs, contributing to glandular impairment, as suggested by Park and Baek, who found a significant correlation between meiboscore and CAS.[4,11] Knop et al[21] suggested that inflammatory mediators could spread and lead to glandular dropout and acinar atrophy by the way of the conjunctiva, through the tarsus and toward the MGs. Although the mechanism underlying MGs inflammation is still unclear, it has been speculated that the increased intraglandular pressure secondary to obstruction might stress ductal and acinar epithelium. This occurrence might trigger proinflammatory protein activity that results in inflammatory response.[21]

As expected, all patients with GO were affected by DED as confirmed by the pathological values of Schirmer

TABLE 1. Demographic and Clinical Parameters of Patients With GO and Control Subjects

Parameter	GO Group	Control Group	*P*
Age (yr)	44.2 ± 9.9	39.8 ± 10.7	0.157
Sex (M/F)	3/18	4/20	0.826
Schirmer test (mm/5′)	4.1 ± 1.0	22.3 ± 3.9	**<0.001**
TBUT (s)	4.3 ± 1.1	12.0 ± 2.7	**<0.001**
Corneal fluorescein staining (Oxford)	1.4 ± 0.6	0.3 ± 0.5	**<0.001**

Significant *P* values (<0.05) are in bold.
M, male; F, female.

TABLE 2. In Vivo Confocal Microscopy Analysis of Meibomian Glands in Patients With GO and Control Subjects

Parameter	GO Group	Control Group	*P*
AUD (U/mm^2)	24.5 ± 8.1	34.2 ± 7.5	**<0.001**
Total gland area (μm^2)	5075.5 ± 2894.7	3395.8 ± 952.4	0.256
TLA (μm^2)	3104.7 ± 1713.3	1393.8 ± 448.0	**0.001**
ALD (μm)	94.4 ± 21.2	64.3 ± 10.1	**<0.001**
ASD (μm)	56.6 ± 15.3	42.2 ± 12.3	**0.001**

Significant *P* values (<0.05) are in bold.

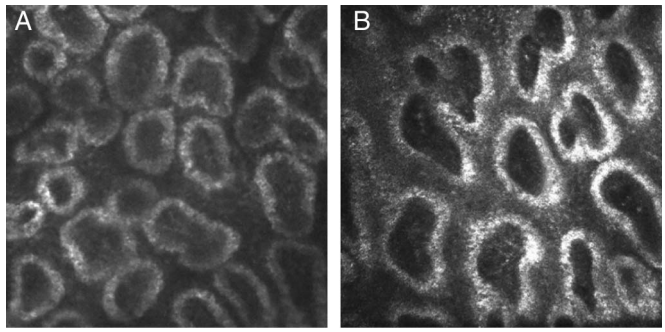

FIGURE 2. Representative IVCM images of MGs in a healthy subject and in a patient with GO (respectively, A and B). A, The mean AUD was 31.3 ± 7.2 U/mm^2. The total gland area and the TLA were, respectively, 5643.5 ± 923.2 μm^2 and 2865.3 ± 1546 μm^2. The mean longest and shortest acinar unit diameters were 69.5 ± 15.1 μm and 40.4 ± 15.2 μm, respectively. B, The mean AUD was 23.6 ± 9.4 U/mm^2. The total gland area and the TLA were, respectively, 5265 ± 876.4 μm^2 and 3872.1 ± 1432.1 μm^2. The mean longest and shortest acinar unit diameters were 92.6 ± 32.3 μm and 58.3 ± 13.2. μm, respectively.

tests and TBUT that were significantly lower compared with controls.

DED is a multifactorial ocular surface disease resulting from damaged tear film homeostasis, in which tear hyperosmolarity, ocular surface inflammation, and neurosensory abnormalities play a pathogenetic role.[23] DED is one of the main conditions occurring in the setting of GO, and recently, MGD has been proposed as a pivotal mechanism of its onset.[24] Under normal conditions, MGs secrete lipids to stabilize the tear film and prevent tear evaporation. Blinking applies a shearing force that lowers the viscosity, making the lipids easier to eject from the gland's orifices.[25]

Interestingly, a recent study conducted on patients with GO reported a thicker LLT in those with severe forms of MGD.[10] The increased value of LLT could depend on both compensatory and stimulatory effects: residual MGs increase lipid production to overcome gland loss; in addition, patients with GO blink more forcefully because of the lid fissure widening, thus making it easier for the lipids to be squeezed out. The aforementioned processes could in turn lead to a vicious stress circle leading to the further impairment of the glands.

Previous reports have investigated IVCM features of MGs in the setting of either primary DED and secondary DED owing to systemic disorders, such as Sjogren syndrome and graft-versus-host disease.[26–28] These studies showed that specific MGs features are exhibited according to each condition, suggesting that the MGs microstructure reflects the underlying pathogenetic process.[26–28]

To the best of our knowledge, this is the first study that describes the MGs microstructure using IVCM.

Our results are consistent with the MGs dropout that was detected in previous reports using both slit-lamp examination and infrared meibography.[4,9–11] The latter technique traditionally assesses in a noninvasive fashion MGs status based on to the percentage of gland dropout. In particular, infrared meibography conventionally explores gland loss because it does not examine the gland itself, but the presence of meibum.[29] Recently, specific algorithms have been applied to meibography examination to provide novel quantitative and qualitative MGs parameters, such as length, width, irregularity, and quality.[12,30–35] However, in previous studies about GO, gland loss was the only parameter evaluated. Thus, the obstructive nature of MGD in this setting was only speculated, based on clinical observations, particularly on the increased palpebral fissure height.[4] Unlike meibography, IVCM allows a microscopic, histology-like visualization of glands with a better resolution and is therefore able to detect also periglandular inflammation along with epithelial hyperkeratinization and basal epithelial density.[36–39] In addition, IVCM allows to directly measure MGs structures, providing a reproducible and precise image evaluation. In GO, glands enlargement detected by IVCM support the hypothesis that obstructive process plays a major role in development of MGD.

Furthermore, as suggested by Randon et al, IVCM allows us to distinguish among different MGD subtypes, namely obstructive, inflammatory, or fibrotic. This, in turn, can help for the choice of the proper treatment for each stage or subtype of the disease.[40] In obstructive MGD, unlike meibography that detected often a mild extent of gland loss, IVCM is the only tool able to detect early histological changes related to the obstruction.[40]

In conclusion, IVCM analysis showed a distinctive pattern of MGs alterations in the setting of GO. Given the meaningful role of MGs in the pathogenesis of DED owing to GO, IVCM can represent a surrogate tool that is able to characterize MGs features at a cellular level.

REFERENCES

1. Smith TJ, Hegedüs L. Graves' disease. *N Engl J Med.* 2016;375: 1552–1565.
2. Garrity JA, Bahn RS. Pathogenesis of Graves' ophthalmopathy: implications for prediction, prevention, and treatment. *Am J Ophthalmol.* 2006;142:147–153.
3. Versura P, Campos EC. The ocular surface in thyroid diseases. *Curr Opin Allergy Clin Immunol.* 2010;10:486–492.
4. Park J, Baek S. Dry eye syndrome in thyroid eye disease patients: the role of increased incomplete blinking and Meibomian gland loss. *Acta Ophthalmol.* 2019;97:e800–e806.
5. Eckstein AK, Finkenrath A, Heiligenhaus A, et al. Dry eye syndrome in thyroid-associated ophthalmopathy: lacrimal expression of TSH receptor suggests involvement of TSHR-specific autoantibodies. *Acta Ophthalmol Scand.* 2004;82:291–297.
6. Gilbard JP, Farris RL. Ocular surface drying and tear film osmolarity in thyroid eye disease. *Acta Ophthalmol (Copenh).* 1983;61:108–116.
7. Iskeleli G, Karakoc Y, Abdula A. Tear film osmolarity in patients with thyroid ophthalmopathy. *Jpn J Ophthalmol.* 2008;52:323–326.
8. Kocabeyoglu S, Mocan MC, Cevik Y, et al. Ocular surface alterations and in vivo confocal microscopic features of corneas in patients with newly diagnosed Graves' disease. *Cornea.* 2015;34:745–749.
9. Kim YS, Kwak AY, Lee SY, et al. Meibomian gland dysfunction in Graves' orbitopathy. *Can J Ophthalmol.* 2015;50:278–282.
10. Wang CY, Ho RW, Fang PC, et al. The function and morphology of Meibomian glands in patients with thyroid eye disease: a preliminary study. *BMC Ophthalmol.* 2018;18:90.
11. Park J, Kim J, Lee H, et al. Functional and structural evaluation of the meibomian gland using a LipiView interferometer in thyroid eye disease. *Can J Ophthalmol.* 2018;53:373–379.
12. Llorens-Quintana C, Rico-del-Viejo L, Syga P, et al. Meibomian gland morphology: the influence of structural variations on gland function and ocular surface parameters. *Cornea.* 2019;38:1506–1512.
13. Ibrahim OM, Matsumoto Y, Dogru M, et al. The efficacy, sensitivity, and specificity of in vivo laser confocal microscopy in the diagnosis of meibomian gland dysfunction. *Ophthalmology.* 2010;117:665–672.
14. Giannaccare G, Pellegrini M, Sebastiani S, et al. In vivo confocal microscopy morphometric analysis of corneal subbasal nerve plexus in dry eye disease using newly developed fully automated system. *Graefes Arch Clin Exp Ophthalmol.* 2019;257:583–589.
15. Wei YH, Chen WL, Hu FR, et al. In vivo confocal microscopy of bulbar conjunctiva in patients with Graves' ophthalmopathy. *J Formos Med Assoc.* 2015;114:965–972.
16. Villani E, Viola F, Sala R, et al. Corneal involvement in Graves' orbitopathy: an in vivo confocal study. *Invest Ophthalmol Vis Sci.* 2010; 51:4574–4578.
17. Bron AJ, Evans VE, Smith JA. Grading of corneal and conjunctival staining in the context of other dry eye tests. *Cornea.* 2003;22:640–650.
18. Wolffsohn JS, Arita R, Chalmers R, et al. TFOS DEWS II diagnostic methodology report. *Ocul Surf.* 2017;15:539–574.
19. Mourits MP, Prummel MF, Wiersinga M, et al. Clinical activity score as a guide in the management of patients with Graves' ophthalmopathy. *Clin Endocrinol.* 1997;47:9–14.
20. Matsumoto Y, Sato EA, Ibrahim OM, et al. The application of in vivo laser confocal microscopy to the diagnosis and evaluation of meibomian gland dysfunction. *Mol Vis.* 2008;14:1263–1271.
21. Knop E, Knop N, Millar T, et al. The international workshop on meibomian gland dysfunction: report of the subcommittee on anatomy, physiology, and pathophysiology of the meibomian gland. *Invest Ophthalmol Vis Sci.* 2011;52:1938–1978.

22. Call CB, Wise RJ, Hansen MR, et al. In vivo examination of meibomian gland morphology in patients with facial nerve palsy using infrared meibography. *Ophthal Plast Reconstr Surg.* 2012;28:396–400.
23. Craig JP, Nichols KK, Akpek K, et al. TFOS DEWS II definition and classification report. *Ocul Surf.* 2017;15:276–283.
24. Kashkouli MB, Alemzadeh SA, Aghaei H, et al. Subjective versus objective dry eye disease in patients with moderate-severe thyroid eye disease. *Ocul Surf.* 2018;16:458–462.
25. Selter JH, Gire AI, Sikder S. The relationship between Graves' ophthalmopathy and dry eye syndrome. *Clin Ophthalmol.* 2015;9:57–62.
26. Giannaccare G, Pellegrini M, Bernabei F, et al. Ocular surface system alterations in ocular graft-versus-host disease: all the pieces of the complex puzzle. *Graefes Arch Clin Exp Ophthalmol.* 2019;257:1341–1351.
27. Kheirkhah A, Coco G, Satitpitakul V, et al. Subtarsal fibrosis is associated with ocular surface epitheliopathy in graft-versus-host disease. *Am J Ophthalmol.* 2018;189:102–110.
28. Fasanella V, Agnifili L, Mastropasqua R, et al. In vivo laser scanning confocal microscopy of human meibomian glands in aging and ocular surface diseases. *Biomed Res Int.* 2016;2016:7432131.
29. Finis D, Ackermann P, Pischel N, et al. Evaluation of meibomian gland dysfunction and local distribution of meibomian gland atrophy by non-contact infrared meibography. *Curr Eye Res.* 2015;40:982–989.
30. Llorens-Quintana C, Rico-Del-Viejo L, Syga P, et al. A novel automated approach for infrared-based assessment of meibomian gland morphology. *Transl Vis Sci Technol.* 2019;8:17.
31. Ban Y, Shimazaki-Den S, Tsubota K, et al. Morphological evaluation of meibomian glands using noncontact infrared meibography. *Ocul Surf.* 2013;11:47–53.
32. Koh YW, Celik T, Lee HK, et al. Detection of meibomian glands and classification of meibography images. *J Biomed Opt.* 2012;17:086008.
33. Koprowski R, Wilczynski S, Olczyk P, et al. A quantitative method for assessing the quality of meibomian glands. *Comput Biol Med.* 2016;75:130–138.
34. Bernabei F, Versura P, Pellegrini M, et al. Longitudinal analysis of infrared meibography in patients undergoing hematopoietic stem cell transplantation. *Cornea.* 2020 [E-pub ahead of print].
35. Giannaccare G, Vigo L, Pellegrini M, et al. Ocular surface workup with automated noninvasive measurements for the diagnosis of meibomian gland dysfunction. *Cornea.* 2018;37:740–745.
36. Alhatem A, Cavalcanti B, Hamrah P. In vivo confocal microscopy in dry eye disease and related conditions. *Semin Ophthalmol.* 2012;27:138–148.
37. Liang H, Randon M, Michee S, et al. In vivo confocal microscopy evaluation of ocular and cutaneous alterations in patients with rosacea. *Br J Ophthalmol.* 2017;101:268–274.
38. Qazi Y, Kheirkhah A, Blackie C, et al. In vivo detection of clinically non-apparent ocular surface inflammation in patients with meibomian gland dysfunction-associated refractory dry eye symptoms: a pilot study. *Eye (Lond).* 2015;29:1099–1110.
39. Zhao H, Chen JY, Wang YQ, et al. In vivo confocal microscopy evaluation of meibomian gland dysfunction in dry eye patients with different symptoms. *Chin Med J.* 2016;129:2617–2622.
40. Randon M, Aragno V, Abbas R, et al. In vivo confocal microscopy classification in the diagnosis of meibomian gland dysfunction. *Eye.* 2019;33:754–760.